EUROPEAN FUSION DEVELOPMENT AGREEMENT

EFDA–JET–PR(01)10

M Groth et al

Helium and Neon Enrichment Studies in the JET MKII AP and MKII GB Divertor

Helium and Neon Enrichment Studies in the JET MKII AP and MKII GB Divertor

M Groth[1,2], P Andrew, W Fundamenski, H Y Guo[3], D L Hillis[4],
J T Hogan[4], L D Horton[5], P D Morgan, G F Matthews, A G Meigs,
M F Stamp, D Stork, M von Hellermann[6].

EURATOM/UKAEA Fusion Association, Culham Science Centre,
Abingdon, Oxfordshire, OX14 3DB, UK.
[1]University of Manchester (UMIST), Manchester, UK.
[2]Present address: Lawrence Livermore National Laboratory/General Atomics,
P O Box 85608, San Diego, CA 92186-5608, USA.
[3]Redmond Plasma Physics Laboratory, University of Washington, Redmond, WA, USA.
[4]Oak Ridge National Laboratory, Oak Ridge, TN, USA.
[5]Max-Planck-Institut für Plasmaphysik, Boltzmannstraße 2, D-85748 Garching, Germany.
[6]FOM Institute for Plasma Physics, Rijnhuizen, Nieuwegein, The Netherlands.

Helium and Neon Enrichment Studies in the JET MKII AP and MKII GB Divertor

M Groth[1,2], P Andrew, W Fundamenski, H Y Guo[3], D L Hillis[4], J T Hogan[4], L D Horton[5], P D Morgan, G F Matthews, A G Meigs, M F Stamp, D Stork, M von Hellermann[6].

EURATOM / UKAEA Fusion Association, Culham Science Centre, Abingdon OX14 3DB, UK
[1] University of Manchester (UMIST), Manchester, UK
[2]Lawrence Livermore National Laboratory/General Atomics, PO Box 85608, San Diego, CA 92186-5608, USA.
[3] Redmond Plasma Physics Laboratory, University of Washington, Redmond, WA, USA
[4] Oak Ridge National Laboratory, Oak Ridge, TN, USA
[5] Max-Planck-Institut für Plasmaphysik, Garching, Germany
[6]FOM Institute for Plasma Physics, Rijnhuizen, Nieuwegein, The Netherlands

ABSTRACT

Adequate helium enrichment and exhaust have been achieved in reactor-relevant ELMy H-mode plasmas in JET performed in the MKII divertor geometry. These quantities, describing the retention of impurities in divertors, have been experimentally inferred from Charge Exchange Recombination Spectroscopy (CXRS) measurements in the core plasma, and from a spectroscopic analysis of a Penning gauge discharge in the exhaust gas. The retention of helium was found to be sufficient with respect to the requirements in a next-step device, with helium enrichment factors exceeding 0.1 in high-density, ELMy H-mode discharges. With increasing core plasma density the helium partial pressure in the exhaust channel increases. While in L-mode plasmas the helium enrichment decreases with increasing core plasma density, it remains almost constant in ELMy H-mode plasma. The noble gas neon is better enriched in the divertor at high core plasma densities in both confinement regimes.

These experimental results can be explained by the significant difference of the penetration depth of the impurity neutrals and their subsequent different impurity transport mechanism. Analytical and numerical analyses of these plasmas using the impurity code package DIVIMP/NIMBUS support the proposition that, due to their much longer ionisation mean free path, helium particles can escape from the divertor chamber as neutrals, while neon escapes by means of ion leakage. Consequently, the divertor plasma conditions strongly influence the noble gas compression and enrichment. Variations of the divertor plasma configuration and modifications to the divertor geometry have enhanced the pumping capabilities of the tokamak, but found not to affect the helium enrichment.

1. INTRODUCTION

In future fusion-relevant devices of significant alpha-particle production, adequate removal of helium is required to maintain core plasma purity and high fusion power. In tokamaks with diverted plasma configurations, the alpha-particle production rate is highest in the centre of the main plasma, and the transport of helium particles to the pumping facilities can be divided into three regions of characteristic transport [1]. Fusion-born helium ions are transported across the magnetic field lines towards the last closed flux surface (separatrix) and into the scrape-off layer (SOL). In the SOL helium ions are rapidly transported along the magnetic field lines into the divertor plasma and onto the divertor target plates. There, helium particles recycle almost perfectly and emerge as neutrals from the target back into the divertor plasma. By means of multiple reflections, a fraction of the helium neutrals eventually enters the pumping chamber where they can be removed by vacuum pumps. The remaining neutral helium particles interact with the divertor plasma and can flow back, either as ions or neutrals, into the main plasma, repeating this cycle many times before eventually being removed.

Correspondingly, the transport processes of deliberately injected noble gases, such as neon and argon, can be described. These gases are chiefly injected into the SOL plasma to disperse, through radiative processes, the large heat fluxes arriving from the core plasma [2]. As noble gases are none-volatile, they generally do not react chemically with the tokamak walls and can, therefore, be more easily controlled via pumping than others radiating gases, like methane or nitrogen. Like helium, these gases need to be confined to the divertor chamber, or at least, to the periphery of the main plasma to maintain sufficient core plasma purity.

In view of divertor operation, a sufficient fraction of impurity particles needs to be retained in the divertor chamber. Additionally, the exhaust of the impurity particles from the tokamak at adequate rates requires a sufficiently large impurity neutral pressure in front of the vacuum pump. The retention efficiency of divertors can be expressed by the figures of the particle compression and impurity enrichment, defined as [3],

$$C_P = \frac{n^0}{n^+} \quad (1)$$

and

$$\eta_{imp} = \frac{C_{imp}}{C_{D-T}} \quad (2)$$

respectively.

The particle compression factor, C_p, expresses the ratio of the neutral density, n^0, measured in the divertor, to the ion density, n^+, determined in the main plasma. To cover all transport processes in a tokamak, the ion density needs to be taken at a central position in the main plasma, e.g. at ρ~0.3. However, this work focuses on SOL transport issues, so that the compression and enrichment factors calculated with respect to the ion densities taken at ρ~0.9 are quoted herein. No direct measurements of the impurity densities in the divertor were performed, so that the neutral densities in the subdivertor are taken instead. As indicated by the shaded area in Fig.1, the subdivertor of the Joint European Torus (JET) is the vacuum region surrounding the lower divertor structure that is not facing the plasma. In particular, this is the region below the divertor target plates and around the vacuum pump. In the subdivertor deuterium and tritium exist in molecular form, the measured neutral density is therefore multiplied by a factor of 2 to calculate their compression appropriately.

To satisfy the requirement of high core plasma purity, while simultaneously keeping the deuterium-tritium (D-T) throughput as low as possible, impurity enrichment factors above unity are desired. According to recent ITER design studies, a dilution of helium particles in the exhaust channel can be tolerated, as long as the helium enrichment factors exceeds 0.1 [4]. Large impurity compression factors are also preferable as they indicate a larger throughput of impurity particles at the pump. Previous investigations of the enrichment of helium in other experimental tokamaks have indicated that these requirements can be met in standard, low-confinement (L-mode) and also in high-confinement (H-mode) discharges [5,6,7,8,9]. At JET helium enrichment factors between 0.1 and unity have been measured [10,11,12]. This work revisits the main findings in JET and interprets them based on a zero-dimensional model and numerical modelling using DIVIMP / NIMBUS [13,14].

2. EXPERIMENTAL CONDITIONS AND ARRANGEMENT

The compression and enrichment of helium and neon in the JET were experimentally determined in impurity gas injection experiments performed in the MKII AP and MKII GB divertor campaign [10,11,12,15]. These pure-deuterium discharges encompassed L-mode and ELMy H-mode plasmas heated with 2MW and 12MW of neutral beam injection (NBI), respectively. Generally, in both L-mode and ELMy H-mode discharges, the core plasma density in these discharges was as such that the divertor plasma was attached to the target plates; only at core plasma densities above $3\cdot10^{19}m^{-3}$ in L-mode plasmas did the divertor plasma partially detach from the target. Helium and neon were injected into the plasma as neutral gas at about midplane (low field side) of the tokamak main chamber, either by puffing or bleeding.

The JET divertor cryogenic pump, installed between the internal divertor coils in the subdivertor chamber (Fig.1), generally operates at liquid helium temperature (4.8K). At this temperature, only deuterium and neon are actively exhausted. This condition permits, however, the thorough study of the sensitivity of the compression and enrichment on unconstrained input parameters, such as the core plasma density. Active helium pumping can be achieved by frosting an argon layer onto the cryo panels [12,16]. As this experimental technique is much more time-consuming, it has only been applied during a series of dedicated discharges in the MKII GB divertor. Under this condition, which is close to that in a future reactor, helium transport and enrichment studies can be performed simultaneously. Unless otherwise stated, the results quoted here refer to the conditions at which helium was not actively pumped.

The core impurity concentration, f_{He}, was measured by charge exchange recombination spectroscopy (CXRS). The JET CXRS system covers the entire core plasma cross-section at approximately midplane and provides measurements at 10 spatial locations, with a time resolution of 50ms [17]. The impurity density profiles of interest were inferred from line intensity measurements of $\Delta n=1$ transitions in the visible wavelength range. These transitions are induced by charge exchange excitation of fully ionised impurity atoms by energetic deuterium beam neutrals. For this study, the de-excitation transitions of HeII $n=4\rightarrow3$ at 468.6nm and NeX $n=11\rightarrow10$ at 524.9nm were used.

The concentration of the impurity neutrals in the subdivertor chamber was assessed by a spectroscopic analysis of light emitted by a Penning gauge [18,19]. As shown in Fig.1, the JET Penning gauge diagnostic encompasses a 3m long vacuum duct mounted at the subdivertor. The light emitted from the gauge's own discharge was relayed through an optical fibre link to a set of photomultipliers. Using interference filters the line emission at the Balmer α-line for deuterium (wavelength 656.1nm/bandwidth 1nm), HeI (587.5nm/2nm) and NeI (640.4nm/1nm) was measured. The system was calibrated over a wide range of pressures (10^{-2}Pa to $5\cdot10^{-1}$Pa total pressure) and impurity concentrations (c_{imp} = 5%-20%), permitting an accurate calculation (Δ~10%) of the partial pressures from the measured line intensities.

3. MEASUREMENT OF THE HELIUM AND NEON COMPRESSION AND ENRICHMENT IN THE JET MKII DIVERTOR

3.1 The effect of the core plasma density on helium and neon enrichment

It was anticipated that the divertor plasma density and temperature are the critical parameters. In JET this dependence was investigated by altering the core plasma density. Moreover, as the core plasma density also represents a main input parameter in future fusion devices, the scaling of the impurity compression and enrichment is therefore crucial knowledge.

The time traces of a typical L-mode discharge (B_T=2.5T, I_p= 2.4MA) performed in the MKII GB divertor are shown in Fig.2. At a constant neutral beam power of 2MW, two different core plasma densities were achieved by increasing the D_2 fuelling rate. At 16s a helium puff of duration 50ms was added, introducing approximately 5×10^{20} helium particles into the plasma. Such relatively large amount of helium in the core plasma, causing f_{He}~15%, was necessary in order to resolve the helium concentration in the subdivertor. The increase in core plasma density was succeeded by an increase of the deuterium and helium compression, as predicted by the Two-Point model [20], while the ratio of partial helium to deuterium pressure in the subdivertor decreases. Subsequently, the helium enrichment deteriorates at larger core plasma densities, to levels of about 0.2 to 0.3.

Results from helium enrichment studies in ELMy H-mode plasmas did not differ greatly from those obtained in L-mode. The HeII concentration profiles were found to be flat and did not indicate any accumulation of helium on-axis [21]. Core plasma densities achieved in H-mode, of the order 5×10^{19} m^{-3}, led subsequently to higher divertor densities and neutral pressures and lower divertor plasma temperatures. The helium enrichment factor does not vary significantly with core plasma density, but in absolute numbers it is smaller compared to that measured in L-mode. Changing the characteristics of the ELMs from type-I to type-III ELMs did not indicate any significant change of the helium enrichment. Experimentally, type-III ELMs have been achieved by increasing the deuterium gas puffing. This led subsequently to slightly different divertor plasma conditions, and the effect of the ELMs could not be discriminated.

Active helium pumping by means of argon frosting resulted primarily in a reduction of the partial helium pressure in the subdivertor chamber. For comparable core and divertor plasma conditions, the helium compression factors were found to be smaller by about a factor of 2, approximately, when both deuterium and helium were actively pumped. For low core-density L-mode plasmas, this difference can be even of the order of 3. Consequently, the helium enrichment factors obtained were also smaller by about a factor of 2 to 3, as shown in Fig.4. For reactor studies it is important to include the core transport in the global transport scheme. For that, the helium enrichment factors are calculated using the core helium concentration at ρ~0.3. In high-density, ELMy H-mode plasmas the helium enrichment measured with respect to the core helium concentration was of the order 0.2, twice the value of 0.1 required in the ITER-FEAT [4]. The helium enrichment factor decreases very modestly with increasing core plasma density.

In contrast to the results obtained by injecting helium, both the compression and enrichment of neon were enhanced as the core plasma density was increased (Fig.3). Typically, the compression of neon was 2 to 3 times larger than the helium compression. The largest neon enrichment factors obtained were of the order 2 in L-mode plasma, while only about unity in ELMy H-mode discharges. The cause of this notable difference is yet not fully understood. Unlike helium, the neon concentration profiles in L-mode and ELMy H-mode differ significantly; in L-mode they were found to be flat to moderately peaked in L-mode, while hollow in H-mode discharges [21]. The neon-to-deuteron ion density ratio taken at ρ~0.9 are consistently larger by a factor of 2 in H-mode. The electron temperature at this location is in well in excess of 500eV, in all L-mode as well as in H-mode discharges. Although the contribution of NeIX was not measured, its contribution can be assumed to be small, due to this high plasma temperature, and cannot describe the significant increase of neon in the plasma edge periphery in H-mode plasmas.

3.2 Efforts to improve the helium compression and enrichment

In order to improve the compression and enrichment of helium, the following experimental methods and divertor configuration modifications were pursued at JET over recent years: (i) varying the divertor plasma configuration, (ii) changing the plasma flow in the SOL, and (iii) increasing the closure of the divertor geometry. The results of these modifications are closely examined herein.

The open geometry of the MKII AP divertor permitted flexible divertor plasma configurations, in which the plasma strike zones can be attached either to the horizontal or vertical target plates, or directly onto the divertor corners (Fig.5). In the course of one L-mode discharge all three configurations were achieved, while simultaneously keeping the core plasma density constant. Helium was injected in a short gas puff, when the first divertor plasma configuration was accomplished. In a series of five 2.7T / 2.5 MA L-mode discharges, each heated with 2MW of NBI, a core plasma density scan was performed. In none of these discharges helium was actively pumped.

It can be demonstrated that the maximum probability for the fuel and impurity neutrals to enter the subdivertor chamber is given in the corner configuration, while the neutrals that leave the vertical target do not see a direct line-of-sight to penetrate the corner slots [22]. Accordingly, the largest partial deuterium and helium pressures were obtained in the corner configuration, resulting in the largest compression factors (Fig.6). As the rate of increase in the compression was almost identical for helium and deuterium, in all three configurations, they all display similar helium enrichment factors.

At DIII-D, a modest improvement of the helium compression and enrichment factor has been observed in ELMy H-mode plasmas, by switching the puff location of the deuterium gas from a divertor to a top location and, thereby, augmenting the ion flow in the SOL plasma [6]. To address this issue at JET, pairs of L-mode discharges were performed in the MKII GB divertor with different deuterium puff locations. In one discharge additional deuterium gas was injected from a gas module at the top of the main chamber, while in the other from a module located in the divertor. As shown in Fig.7, the core plasma density and the core HeII concentration were matched, however, the subdivertor neutral pressure is significantly higher at high core plasma density, when deuterium is puffed in the divertor. The variation of the helium compression and enrichment measured is small and could be due to this difference in the neutral subdivertor pressure. However, this observation could also be due to the strong, intrinsic SOL flow as measured at JET [23], that might not be much altered by additional deuterium gas puffing, or due to different neon fueling of the SOL and divertor plasma. A conclusive answer to this question could not been deduced from the data in hand.

Restricting the escape routes of neutrals into the main chamber, as previously performed in the upgrade from the MKI to the MKIIA divertor, the divertor neutral density was increased for otherwise similar core plasma conditions. Closing the divertor lead therefore to an enhancement of the tokamak's pumping capabilities [24]. In a further upgrade of the MKII divertor structure, the divertor volume was once more restricted, giving it a "deep" W-structure. The latter divertor modification to the MKII divertor is illustrated in Fig.8, showing the previously installed MKII AP divertor and the currently used MKII GB divertor. Resulting from that, the neutral density in the subdivertor was once more increased, by a factor of 2 to 3, for otherwise similar core plasma conditions [11,15].

As shown in Fig.9, in L-mode discharges the increase in the neutral helium pressure in the subdivertor subsequently resulted in an increase of the helium compression. In contrast, such increase was not observed in ELMy H-mode, even though a similar increase in the partial helium pressure was seen. The deuterium compression was also increased, at similar rates, resulting in virtually the same helium enrichment factors in both divertor geometries. A more closed divertor permits, therefore, better helium pumping, but does not improve the enrichment of helium in the divertor.

4. ANALYTIC MODEL FOR THE LEAKAGE OF IMPURITY NEUTRALS

The opposite behaviour of the helium and neon enrichment suggests that their leakage from the divertor into the main chamber is fundamentally different. Impurities released as neutrals from the divertor target plates can either escape directly into the main plasma as neutrals, or become ionised and are transported as ions upstream along the magnetic field lines. To distinguish which means of transport dominates, the ionisation mean free path of the impurity and D/T neutrals can be used as the critical parameter. For simplicity, one can assume that neutrals are ionised in a plasma of density n_e and temperature T_e by electron impact only, so that the ionisation mean free path, $\lambda_{n\text{-}e}$, is readily written as

$$\lambda_{n-e} = \frac{v_0}{n_{e,div}\langle\sigma \cdot v_e\rangle} \tag{3}$$

where v_0 is the velocity of the neutrals and $<\sigma v_e>$ the ionisation rate coefficient, an implicit function of plasma temperature.

To make a comparison between the ionisation mean free paths of helium, neon and D/T atoms, the divertor plasma is herein regarded as box of constant density and temperature. As under typical JET divertor conditions, i.e. $n_{e,d} \sim 5\times10^{19}m^{-3}$, $T_{e,d} \sim 10eV$, the impact energies are well above 50eV, the particle reflection coefficient of helium and neon is significantly less than unity, so that most of the impurity particles are released from the divertor walls by thermal desorption [25]. Thus, these neutrals carry characteristically the (thermal) temperature of the target plates, approximately 0.02eV. Analogously, the region where the ionisation of the D/T atoms takes places can be defined. However, most of the D-T molecules (D-D, T-T, equivalently) are subject to Franck-Condon dissociation. Due to the break-up and subsequent charge exchange with other deuterium or tritium atoms, their kinetic energy is much larger, of order 2-3eV [26].

Using these approximations, an ionisation mean free paths of typically a few centimetres is computed for emerging helium and deuterium atoms, while neon is already ionised within a few millimetres. Depending on the size of the divertor plasma, the likelihood for helium escaping from the divertor in its neutral state is much larger than for neon. Under typical JET divertor conditions, the divertor plasma temperature exerts greater influence on the ionisation mean free paths than the divertor plasma density, causing $\lambda_{n\text{-}e}$ to be longer even when the density is increased. Within the validity of the simple model described, this might be the cause of the different core plasma density dependence of the helium and neon enrichment factors. The leakage of impurity neutrals and ions are therefore treated separately in the following sections.

4.1 Divertor neutral model and neutral impurity leakage

As shown above, helium particles are very likely to escape from the divertor plasma as neutrals. They are therefore not bound to the magnetic field lines, but travel on straight lines until they are ionised or reflected on the vessel walls. To describe the compression and enrichment of helium, a simple, zero-dimensional treatment of the incoming flow of plasma and outgoing flow of neutrals has been used [27] and is extended herein. Divertor geometry effects are neglected.

As illustrated in Fig.10, the flow of ions of any plasma species is approximated to a stream of particles from the main chamber into the divertor volume. The partition of the main to the divertor chamber is chosen arbitrarily, here at the x-point location, approximating the extent of the divertor plasma. The plasma flow is given by the product of ion density, n^+, the flow velocity, v^+, and the effective SOL area at the x-point, A_u,

$$\Gamma^+ = n^+ v^+ A_u \tag{4}$$

In JET, helium and neon were found to recycle almost perfectly, with negligible retention in the target plates. Hence, the flow of ions onto the target, Γ^+_{target}, is therefore balanced by an equivalent flow of neutrals emerging from the surface,

$$\Gamma^+_{target} = \Gamma^0 = n^0 v^0 A_d \tag{5}$$

where $n^0$and v^0 are the neutral density and velocity, respectively. The parameter A_d expresses the plasma-wetted area at the target. Neutral particles leaving the target area can reach the main chamber with a probability P_{back}, or they are ionised within the divertor plasma and return to the target plate, repeating the cycle many times. Neutral particles can also enter the subdivertor chamber via the divertor corner slots, with a probability P_{pump}, from where they are removed. In this model no fueling of the main plasma from the subdivertor volume is assumed. In steady-state, the in- and outflow in the divertor chamber is balanced, yielding,

$$\Gamma^+ = \left[\left(1 - P_{pump}\right) P_{back} + P_{pump}\right] \Gamma^+_{target} \tag{6}$$

Simulations using DIVIMP/NIMBUS, as presented in section 5, have shown that the neutral flow into the subdivertor is small, of the order 5% of the total neutral flux onto the walls. Thus, the particle compression, C_p, can be simplified to

$$C_P = \frac{n^0}{n^+} = \frac{1}{P_{back}} \cdot \frac{v^+}{v^0} \tag{7}$$

using Eqn.4, 5 and 6.

As this model treats neutral flow only, there is no ion transport upstream. The ion flow velocity into the divertor is furthermore assumed to be the same for each plasma species, i.e. $v_{imp}^+ \approx v_D^+$. Hence, the particle compression of impurity and D/T atoms, Eq.6, can be combined to express the enrichment factor as

$$\eta_{imp} \approx \frac{P_{back,D/T}}{P_{back,imp}} \cdot \frac{v^0_{imp}}{v^0_{D/T}} \tag{8}$$

The probability of neutrals returning to the main chamber can be related to the ionisation mean free path via an exponential, i.e. $P_{back} \propto \exp(-L_{div}/\lambda_{n\text{-}e})$. As illustrated in Fig.10, the parameter L_{div} denotes a characteristic length of the divertor. This parameter is of great significance, as it is contained in an exponential function. Unfortunately, very little is known about this parameter, so that it is approximated to the depth of the divertor, at JET about 10cm. The impurity enrichment factor then yields the following proportionality,

$$\eta_{\text{imp}} \propto \exp\left(\frac{L_{\text{div}}}{\lambda_{\text{n-e,D/T}} \cdot \lambda_{\text{n-e,imp}}} \cdot \left(\lambda_{\text{n-e,D/T}} - \lambda_{\text{n-e,imp}}\right)\right) \tag{9}$$

or, more generally,

$$\eta_{\text{imp}} \propto \exp\left(\lambda_{\text{scal}}\left(L_{\text{div}}, \lambda_{\text{n-e,imp,}}, \lambda_{\text{n-e,D/T}}\right)\right) \tag{10}$$

where λ_{scal} is the exponent of the exponential given in Eq.9. Thus, as the distance between the ionisation fronts of the impurity and D/T atoms becomes shorter, so the impurity enrichment decreases. Also, the longer the ionisation mean free path, the smaller the enrichment factor. Experimentally, enlarging the divertor plasma, i.e. increasing L_{div}, will make the divertor plasma more opaque to impurity neutrals and improve the impurity enrichment. The consequences of this model with respect to the experimental results are discussed in section 5.

4.2 Neuhauser Model and Ion Impurity Leakage

The leakage of impurity ions has been formerly explained in a one-dimensional ion transport model suggested by Neuhauser [28]. In this model the main mechanism enabling and supporting the retention of impurities in the divertor chamber is provided by the friction between the ambivalent plasma flow of the background plasma species (to the target) and impurity ions (from the target). This friction force is mainly counteracted by the forces arising due to temperature gradients in the SOL plasma. Impurity neutrals with short ionisation mean free paths emerge from the target plates and are ionised well within the region where the background flow is still strong.

According to a detailed analysis of the Neuhauser model, the impurity density at an upstream position of the SOL, $n^+_{imp,u}$, can be related to the location where the impurity neutrals are ionised, $n^+_{imp,d}$, leading to the following expression [29],

$$\frac{n^+_{\text{imp,u}}}{n^+_{\text{imp,d}}} \propto \exp\left(-\frac{n^+_{\text{D/T,d}} Z^2}{T^2_{\text{D/T,d}}} \Delta s\right) \tag{11}$$

Here, the distance between the ionisation mean free path of the D/T and impurity neutrals is denoted by Δs, Z is the charge state of the impurity ion, and $n^+_{D/T,d}$ and $T_{D/T,d}$ are the density and temperature of divertor plasma, respectively. According to Eq.11, the greater Δs, the more effective the retention of impurity ions in the divertor. Impurity ions with short ionisation mean free path will therefore be more effectively retained in the divertor.

The divertor plasma conditions of the working gas can be related to the upstream SOL plasma density, $n^+_{D/T,u}$, by using the Two-Point model [20]. For a high-recycling SOL plasma, this is given by $n^+_{D/T,d} \propto (n^+_{D/T,u})^3$ and $T_{D/T,d} \propto (n^+_{D/T,u})^{-2}$. Thus, the upstream-to-downstream impurity density ratio can be written as,

$$\frac{n^+_{\text{imp,u}}}{n^+_{\text{imp,d}}} \propto \exp\left(-\left(n^+_{\text{D/T,u}}\right)^7 Z^2 \Delta s\right) \tag{12}$$

Defining an impurity enrichment factor, that is solely due to ion transport, η^{+}_{imp},

$$\eta^{+}_{imp} := \left(\frac{n^{+}_{imp,d}}{n^{+}_{imp,u}}\right) \Big/ \left(\frac{n^{+}_{D/T,d}}{n^{+}_{D/T,u}}\right) \tag{13}$$

would therefore yield

$$\eta^{+}_{imp} \propto \frac{\exp\left(\left(n^{+}_{D/T,u}\right)^{7} Z^{2} \Delta s\right)}{\left(n^{+}_{D/T,u}\right)^{2}} \tag{14}$$

For the divertor plasma conditions given, the nominator of Eq.14 dominates the equation. Thus, larger impurity enrichment factors are achieved at higher core plasma density, provided the impurity neutrals are ionised well within the recycling zone of D/T. This analytic result does indeed describe the experimentally-observed density dependence of the neon enrichment.

The comparison of the two transport mechanisms leads therefore to the important conclusion that ion leakage would be preferable to neutral leakage. Divertor plasmas should be hot enough to ionise impurity particle well within the divertor.

5. COMPARISON OF EXPERIMENTAL RESULTS WITH THE NEUTRAL DIVERTOR MODEL AND TWO-DIMENSIONAL MODELLING USING DIVIMP/ NIMBUS

Following the analytic description given in section 4, the compression and enrichment of impurities in the divertor are closely related to the divertor plasma density and temperature. In JET, these parameters are measured by a fixed set of Langmuir probes mounted at the divertor target plates and varied in the experiments described between 1×10^{19}-$5\times10^{19}m^{-3}$ and 30-5eV, respectively. Using the Langmuir probe measurements and simplifying the divertor plasma to a box of constant plasma density and temperature, the ionisation mean free paths range from 3-5cm for deuterium, 2-4cm for helium, and 2-8mm for neon atoms. Most importantly, the ionisation mean free paths increase with increasing core plasma, thus divertor plasma density. This strongly indicates that it is the temperature is the crucial parameter that determines the penetration depth of neutrals under the plasma conditions regarded. Substituting the ionisation mean free paths into Eq.9, the scaling given by the divertor neutral model can then be compared to the impurity enrichment factors obtained in the experiments. This comparison is shown in Fig.11, using the exponent of Eq.10 as the scaling parameter, λ_{scal}. Larger impurity enrichment factors are predicted by the divertor neutral model for greater values of λ_{scal}, following the trend of measurements. For λ_{scal} values greater than 30 the experimentally obtained enrichment factors deviate from the scaling, indicating the limit of the divertor neutral model and revealing that the leakage mechanism has changed and become governed by the impurity ions. This would be the case of neon at high core plasma density, when its ionisation mean free path becomes completely negligible compared to that of deuterium.

To include the variations of the divertor background plasma conditions and to implement the full divertor geometry, the helium and neon injection experiments have been simulated using the two-dimensional code package DIVIMP/NIMBUS [13,14]. Using DIVIMP/NIMBUS, one impurity species per run was injected into a previously determined background plasma at about midplane of the main chamber. A constant perpendicular diffusion coefficient of $0.1m^2s^{-1}$ and a zero pinch velocity were ascribed to all impurity ions. Impurity ions, which have crossed the outermost ring of the numerical grid, were allowed either to diffuse back to the plasma, or they are lost to a specific target area. Here, the characteristic time scale by which the ions are lost to the target was approximated to 10^{-3}s [29]. The recycling of helium and neon at the divertor target was simulated by re-injecting these particles in a cosine velocity distribution of energy 0.02eV, corresponding to the divertor target temperature of 200K. As DIVIMP does not follow impurity particles into the pumping chamber, a simple neutral transport model was applied to derive the partial impurity and deuterium pressure at a location corresponding to that of the Penning gauges. A series of L-mode discharge simulations in the MKII AP and MKII GB divertor were performed for various target conditions and divertor plasma configurations.

Helium and neon compression and enrichment factors were obtained from the partial impurity to deuterium pressure ratio obtained in the subdivertor chamber, and the impurity to electron density ratio of the fully stripped impurities. Reference point for the latter parameter was the outboard midplane position on the computational mesh ring that represents the separatrix.

The average ionisation mean free paths obtained from DIVIMP/NIMBUS vary between 3cm for deuterium, 2cm for helium and 5mm for neon atoms, with only little dependence on the upstream density. Regarding the neutral and ion transport together, the impurity compression and enrichment factors vary significantly with upstream density, as shown in Fig.12. When increasing the upstream density in the simulation, the ratio of the helium to deuterium neutral density in the subdivertor decreases, while the ratio of the neon to deuterium neutral density moderately increases. Subsequently, the helium and neon enrichment responded oppositely to changes in the core plasma density.

The absolute values of the numerical results are sensitive to the set-up parameters, in particular to the characteristic ion loss time of the far periphery target and the re-injection energy of the impurity neutrals. Both parameters were therefore systematically scanned. The sensitivity scans showed that the compression and enrichment factors inferred from DIVIMP/NIMBUS simulations can differ by a factor of 5; still preserving the density dependence of the impurity compression and enrichment.

The comparison of the results from JET MKII AP and MKII GB divertor using DIVIMP/NIMBUS numerically confirmed the greater particle exhaust in the more closed MKII GB divertor geometry, while the enrichment factors are virtually the same in both divertor geometries. Similarly, DIVIMP/NIMBUS simulations of the various divertor plasma configurations showed no significant variations in the helium enrichment factor.

6. CONCLUSIONS

Helium and neon compression and enrichment have been studied both experimentally and numerically, with the view on their core plasma density dependence in the various JET divertor plasma configurations and geometries.

The study of the compression and enrichment of helium in L-mode discharges has shown an increase in the compression factor at larger core plasma densities, while its enrichment decreases with increasing core plasma density. In ELMy H-mode discharges, the helium compression and enrichment show very little variation with core plasma density. Neither the divertor plasma configuration nor the divertor geometry did affect the enrichment of helium significantly. In high-density ELMy H-mode discharges in the MKII GB divertor geometry, the helium enrichment was found to be marginally above a value of 0.1, as required from the reduced-cost ITER design study [3]. In comparison, in L-mode discharges the enrichment of neon was better at large core plasma densities, exhibiting enrichment factors of up to 2.5.

These experimental results indicate that the enrichment of noble gases is determined by the penetration depth of the impurity neutrals into the divertor plasma. Depending on the background plasma conditions, divertor leakage is either dominated by neutral or ion transport processes. This explanation is supported by an analytic analysis of the neutral and ion flows in the divertor, and by detailed DIVIMP/NIMBUS simulations. From the divertor neutral model it can be shown that helium escapes preferentially as a neutral, hence it is necessary to ionise the helium atoms before they can enter the main chamber. A divertor with a greater plasma volume would offer the prospect of improving the helium retention capabilities of a future fusion facility. In ITER-FEAT [3], with its divertor plasma dimension 2 to 3 times larger that in JET, it can be expected that helium is indeed ionised within the divertor plasma, so that the enrichment should be above the required minimum and improve with density.

ACKNOWLEDGEMENTS

This work has been conducted under the JET Joint Undertaking and is partly funded by Euratom and the UK Department of Trade and Industry. Furthermore, the authors gratefully acknowledge the support from P.C. Stangeby regarding the modelling aspect using DIVIMP/NIMBUS.

REFERENCES

[1] Reiter, D. et al., Nucl. Fusion **30**, (1990) 2141.
[2] Post, D.E. et al., J. Nucl. Mater **220**, (1995) 143.
[3] Janeschitz, G., ITER-JCT and Home Teams, Plas. Phy. Contr. Fusion, **37**, (1995) A19.
[4] Kukushkin, A. et al., in Contr. Fusion Plas. Phy. (Proceedings of the 26th EPS Conference, Maastricht), **23J**, (1999) 1545.
[5] Wade, M.R., J. Nucl. Mater. **220-222**, (1995) 178.
[6] Wade, M.R., Nucl. Fusion **38**, (1998) 1839.
[7] Goetz, J.A. et al., J. Nucl. Mater. **266-269**, (1999) 354.
[8] Bosch, H.-S., in Hogan, J.T. and Hillis, D.L., Nucl. Fusion **40**, (2000) 879.

[9] Sakasai, A. et al., J. Nucl. Mater. **266-269**, (1999) 312.

[10] Groth, M. et al., in Contr. Fusion Plas. Phy. (Proceedings of the 25th EPS Conference, Prague), **22C**, (1998) 39.

[11] Guo, H.Y. et al., Nucl. Fusion **40**, (2000) 379.

[12] Stork, D. et al., in Control. Fusion Plas. Phy. (Proceedings of the 26th EPS Conference, Maastricht), **23J**, (1999) 205.

[13] Stangeby, P.C. et al., Nucl. Fusion **35**, (1995) 1391.

[14] Cupini, E. et al., NET XII-324/9 Report, *NIMBUS – Monte Carlo Simulation of Neutral ParticleTransport in Fusion Devices*, Brussels, (1984)

[15] Monk, R.D. et al., Nucl. Fusion **11Y**, (1999) 1751.

[16] Papastergiou, S., JET Report JET-P(94), *The JET In-Vessel Divertor Cryopump Design, Manufacture, Assembly, Testing and Operational Safety*, **35**, JET Joint Undertaking, Abingdon, (1994).

[17] von Hellermann, M. et al., *Active Beam Spectroscopy in JET* in *Atomic and Plasma-Material Interaction Processes in Controlled Thermonuclear Fusion*, Ed. Janev, R.K. and Darwin, H.W., Elsevier Science, Amsterdam, (1993) 142.

[18] Hardtke, A., Ph.D. thesis, *Entwicklung eines Messverfahrens f¸r die Helium-Partialdruckbestimmung in Gegenwart von Deuterium*, University of Essen, (1989).

[19] Finken, K.-H. et al., Rev. Sci. Instrum. **63**, (1992) 1.

[20] Stangeby, P.C., McCracken, G.M., Nucl. Fusion **30**, (1990) 1225.

[21] von Hellermann, M., in Hogan, J.T. and Hillis, D.L., Nucl. Fusion **40**, (2000) 879.

[22] Loarte, A. et al., in Contr. Fusion Plas. Phy. (Proceedings of the 24th EPS Conference, Berchtesgarden), vol. **21A III**, (1997) 1049.

[23] Erents, S.K. et al., Plas. Phy. Contr. Fusion **42**, (2000) 905.

[24] Vlases, G.C. at al., J. Nucl. Mater. **266-269**, (1999) 160.

[25] Eckstein, W. et al., in *Atomic and Plasma-Material Interaction Data for Fusion*, Nucl. Fusion Special Issue, edited by Janev, R.K., IAEA Vienna, (1991).

[26] Janev, R.K. et al., *Elementary Processes in Hydrogen-Helium Plasmas*, Springer Verlag Berlin, (1987).

[27] Ullrich, W., Ph.D. thesis, *Helium Transport in der Plasmarandschicht an ASDEX Upgrade*, University of Augsburg, (1999).

[28] Neuhauser, J. et al., Nucl. Fusion **24**, (1984) 39.

[29] Stangeby, P.C., *The Plasma Boundary of Magnetic Fusion Devices*, IoP Bristol, (2000) 316.

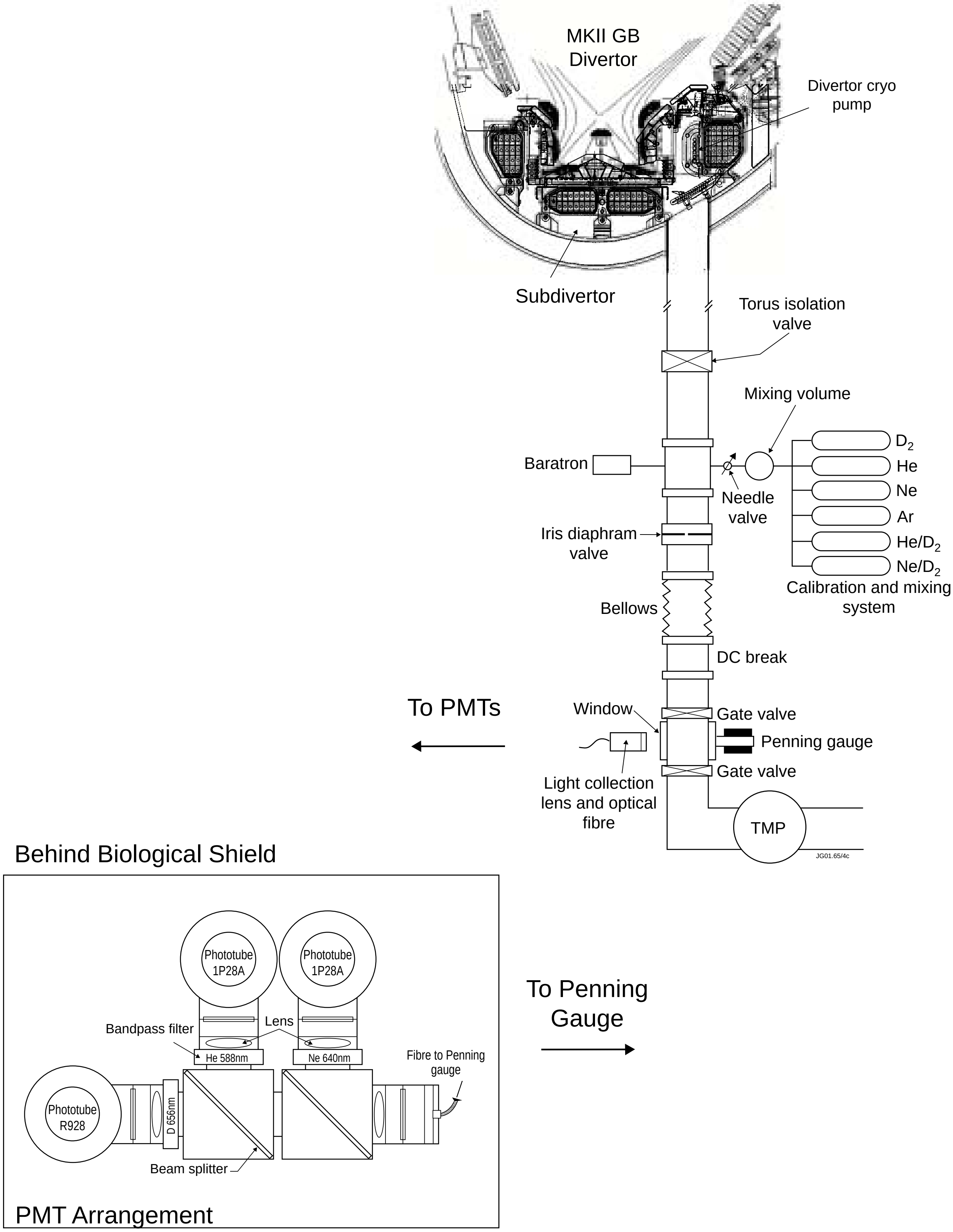

Fig.1: Illustration of the JET Penning gauge diagnostic and the photomultiplier arrangement for the simultaneous line intensity measurement of the deuterium Balmer-α (656.1nm), He I (587.5nm) and Ne I (640.4nm) transitions.

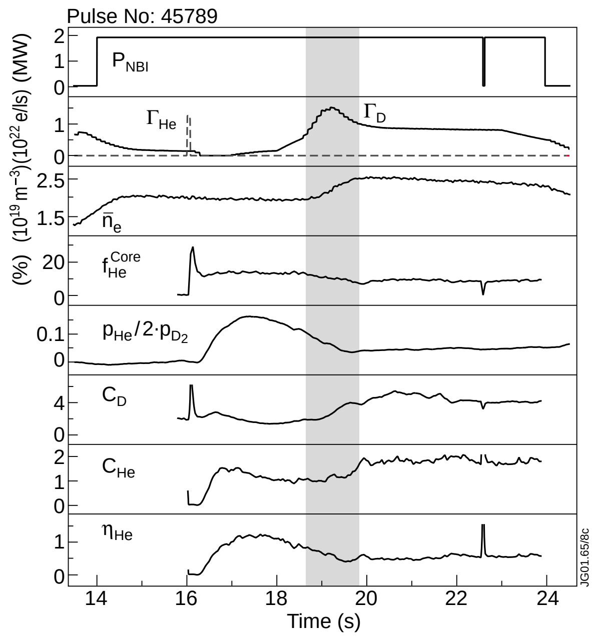

Fig.2: Time traces of a 2.5T/2.4MA L-mode discharge with helium injection at 16s. The traces shown are the injected heating power (NBI), the deuterium and helium gas injection rate, the core plasma density, the core helium concentration, the partial helium to deuterium pressure ratio, the deuterium and helium compression and the helium enrichment factor. The shaded area indicates the change from one density plateau to the other.

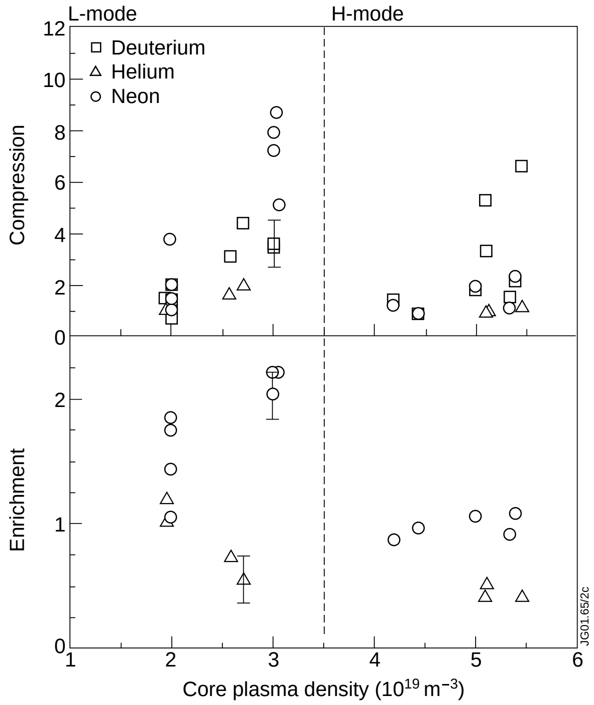

Fig.3: Compression and enrichment factor for deuterium, helium and neon measured in L-mode and ELMy H-mode plasmas in the MKII GB divertor geometry.

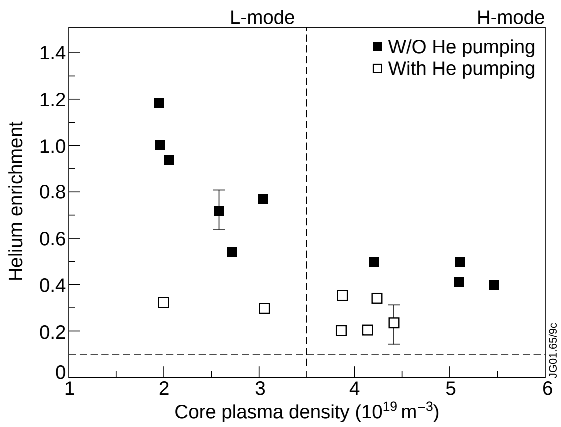

Fig.4: Effect of active helium pumping on the helium enrichment (MKII GB divertor geometry). The helium enrichment factors were determined w.r.t. f_{He} at ρ~0.3. Helium enrichment factors larger than 0.1 are required in ITER-FEAT [4].

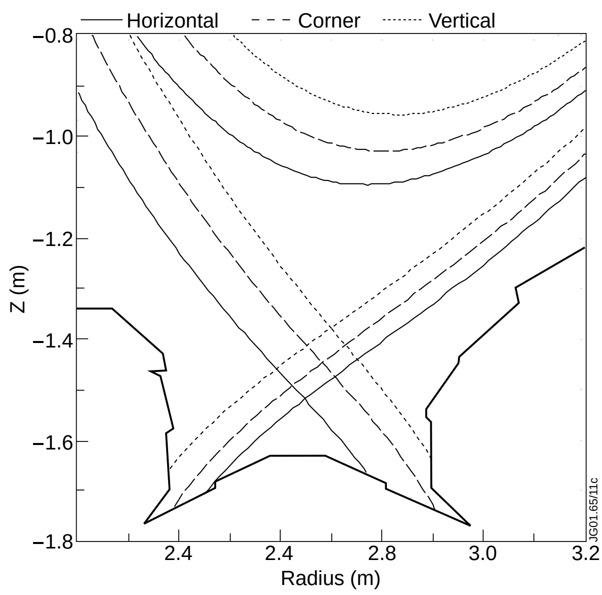

Fig.5: Magnetics of the horizontal, corner and vertical divertor plasma configuration in the MKII AP divertor geometry.

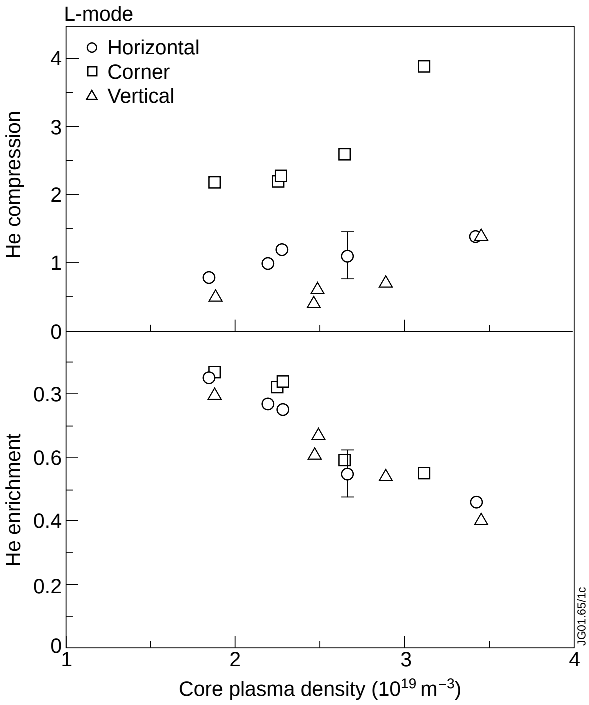

Fig.6: Helium compression and enrichment factors measured for L-mode plasmas in the horizontal, corner and vertical divertor plasma configuration in the MKII AP divertor geometry.

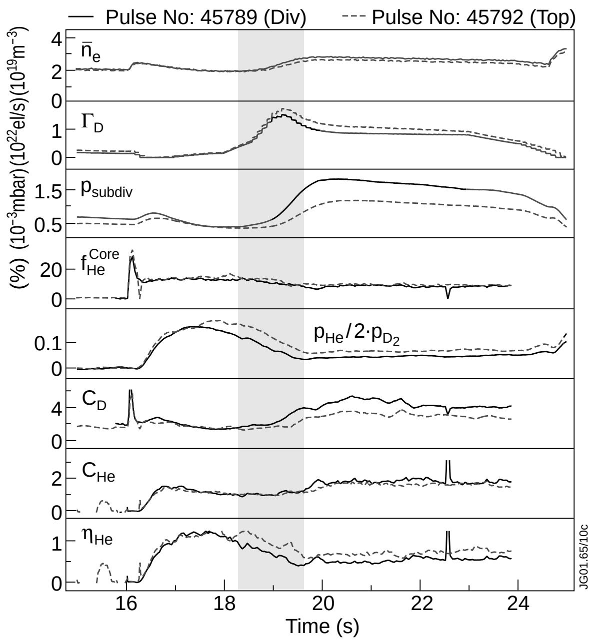

Fig.7: Effect of the deuterium gas fuelling location on helium compression and enrichment (L-mode, MKII GB divertor). The time traces shown are the core plasma density, the deuterium gas injection rate, the subdivertor pressure, the core helium concentration, the partial helium to deuterium pressure ratio, the deuterium and helium compression and the helium enrichment factor. The shaded area indicates the change from one density plateau to the other.

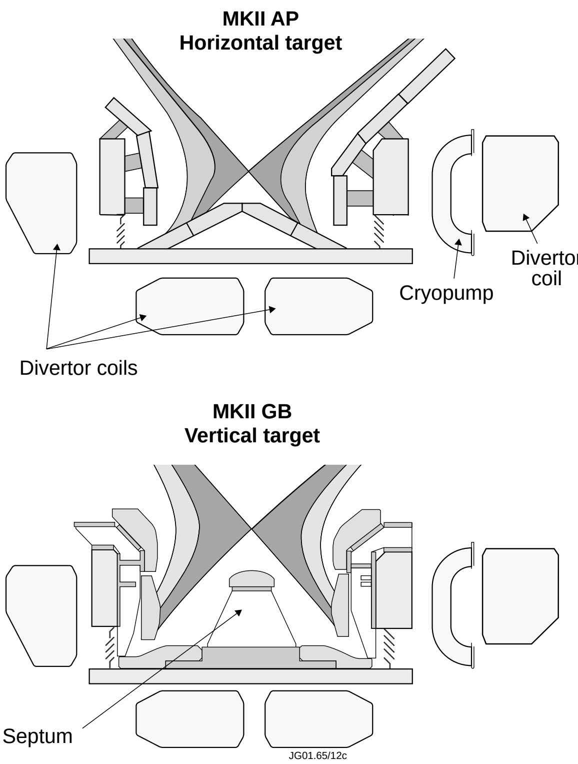

Fig.8: Poloidal cross-sections of the MKII AP and MKII GB divertor geometry.

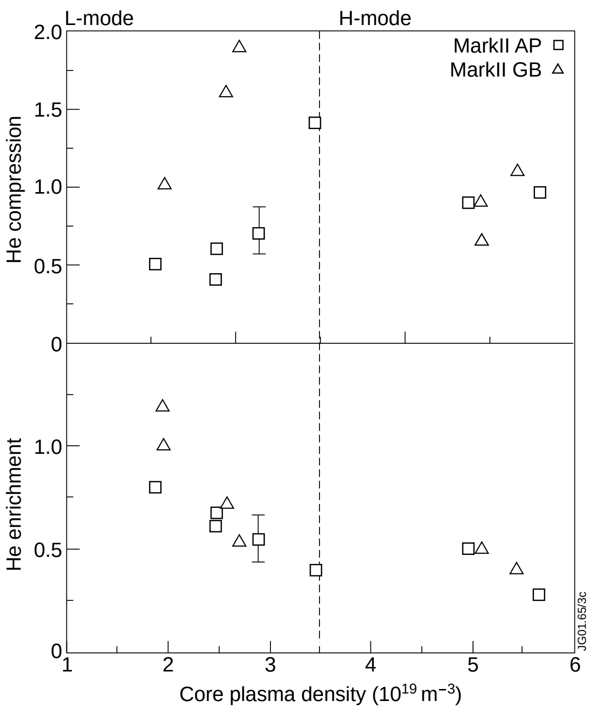

Fig.9: Helium compression and enrichment factors measured in L-mode and ELMy H-mode plasmas in the MKII AP and MKII GB divertor geometry.

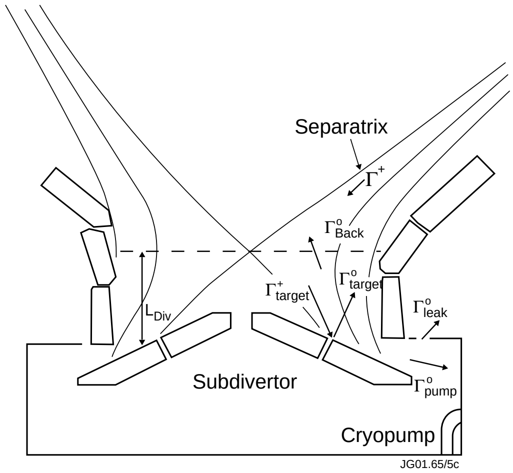

Fig.10: Schematic view of the divertor neutral model to explain divertor retention by means of neutral escape.

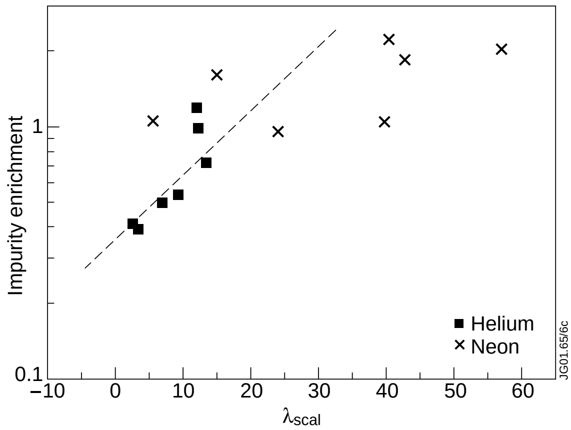

Fig.11: Comparison of the experimentally obtained impurity enrichment factors (points) with the scaling given by the divertor neutral model (dashed line) for L- and ELMy H-mode discharges. The scaling parameter, λ_{scal}, is given by the exponent of the exponential function (Eq.10).

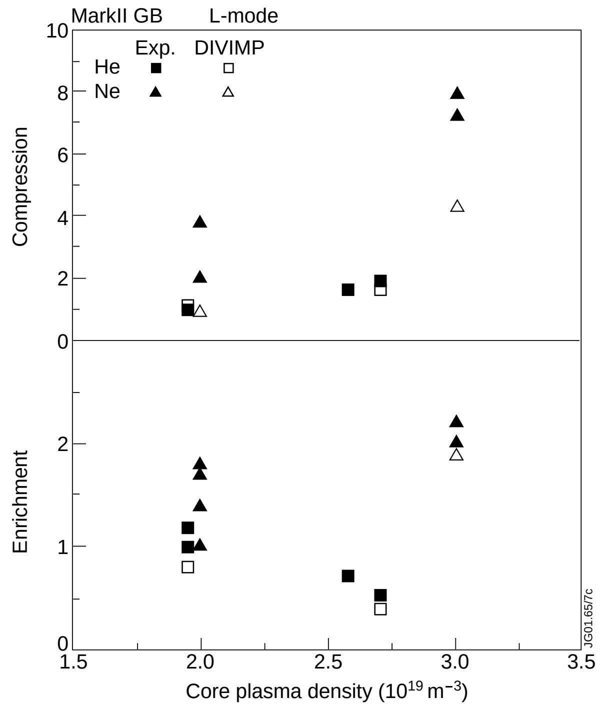

Fig.12: Comparison of the measured impurity compression and enrichment factors with numerical results obtained from DIVIMP/NIMBUS [13,14] for L-mode discharges in the MKII GB divertor geometry.